AIAA JOURNAL
Vol. 37, No. 7, July 1999

Viscous Drag Reduction Using Riblets on a Swept Wing

S. Sundaram,* P. R. Viswanath,† and N. Subaschandar*
National Aerospace Laboratories, Bangalore 560 017, India

Results of viscous drag reduction using 3M riblets on a swept wing with a general aviation wing (GAW)(2) airfoil section at low speeds are presented. The tests, made at a chord Reynolds number of 0.75×10^6, covered an incidence range of 0–6 deg. Measurements consisted of surface-pressure distributions and total drag using wake survey over the range of incidence covered; in addition, mean velocity, streamwise turbulence intensity, and Reynolds shear-stress profiles in the boundary layer were measured just ahead of the trailing edge at zero incidence. Surface flow patterns on the wing were obtained using an oil-flow technique employing titanium dioxide as pigment. The results showed viscous drag reduction of about 8% at zero incidence, which decreased progressively to about 1% at an incidence of 6 deg. The fall in riblet effectiveness appears to be a result of significant riblet yaw-angle effects observed at higher incidence. Some reduction in the turbulence intensity and Reynolds shear stress in the boundary layer on the wing's upper surface have been observed in the presence of riblets, as in two-dimensional flows.

Nomenclature

C_{DT} = sectional total drag coefficient, drag force/$(q_\infty \times c)$
C_p = static-pressure coefficient
c = wing chord, 450 mm
f = frequency, Hz
h = riblet height
h^+ = Reynolds number based on $h = (hu_\tau)/\nu$
p = wall static pressure
q_∞ = freestream dynamic pressure
U_∞ = freestream velocity
u = local mean velocity in the streamwise direction
$\langle u' \rangle$ = rms of velocity fluctuation in the streamwise direction
$\langle u'v' \rangle$ = rms of Reynolds shear-stress component in the streamwise direction
u_τ = friction velocity
$\langle v' \rangle$ = rms of velocity fluctuation in the direction normal to the tunnel axis
x = distance along the airfoil chord, from the leading edge
y = distance normal to tunnel axis
z = distance in the lateral direction
α = angle of attack
β = Clauser pressure-gradient parameter, $(\delta^*/\tau_w)(dp/dx)$
ΔC_{DT} = $C_{DT\,rib} - C_{DT\,smooth}$
δ^* = boundary-layer displacement thickness
ν = kinematic viscosity
τ_w = wall shear stress
φ = local angle between surface streamline and riblet orientation (see Fig. 9): also referred to as *riblet yaw angle*

I. Introduction

THE past decade has seen significant interest and research in the broad subject of viscous drag reduction, and the use of riblets has been most promising so far.[1–4] Plastic riblet films with symmetric v grooves manufactured by the 3M Company, United States, have been widely used in research. The effectiveness of riblets in reducing drag of simple two-dimensional configurations is fairly established now[1–8]; viscous drag reduction in the range of 4–8% at zero incidence has been reported from both wind-tunnel and flight tests. Sundaram et al.[5] reported a monotonically increasing trend of drag reduction with incidence on a NACA 0012 airfoil model at low speeds; viscous drag reduction, as high as 16%, was observed at an incidence of 6 deg, corresponding to a Clauser parameter β of 1.6 for the upper surface-pressure distributions. They also showed that the higher drag reduction with incidence resulted primarily from the airfoil upper (or suction) surface, suggesting an increased effectiveness of riblets in adverse pressure gradients. In a subsequent work, Subaschandar et al.[6] extended the studies of Sundaram et al.[5] to higher angles of attack (using the same NACA 0012 model and in the same wind tunnel); their results showed that both viscous and total drag reduction decreased rapidly beyond $\alpha = 6$ deg, possibly because of the boundary layer on the upper surface approaching separation. Qualitatively similar results, over the range of α up to stall, were reported by Subaschandar et al.[7] on a general aviation wing (GAW)(2) airfoil as well.

In the context of swept wings, very few studies have been reported on riblet effectiveness. Mclean et al.[9] found average total drag reduction of about 6% at cruise condition in a flight experiment on a T-33 jet trainer, which has a wing sweep of about 5 deg. These experiments were made on a glove carrying 3M riblets (with $h = 0.0325$ and 0.075 mm) under 15 different flight conditions (speeds and altitudes). The riblet performance on an ONERA-D airfoil section infinitely swept at 22.5 deg and at zero incidence was reported by Coustols[10]; total drag reduction of about 6% was found using the wake survey method at a chord Reynolds number of 0.5×10^6. The preceding two studies show that the riblets are effective on a swept wing at zero (or low) wing incidence, but virtually no information exists on the effect of incidence on drag reduction or on aspects of boundary-layer development affected by riblets. Unlike a two-dimensional airfoil, additional features due to the crossflow boundary layer and associated riblet yaw-angle effects could be important on a swept wing.

The present work is an attempt to investigate in some detail the effectiveness of 3M riblets and aspects of flow features on an infinite swept wing at low speeds covering airfoil incidence ranging up to 6 deg; the GAW(2) profile has been chosen because of strong practical relevance, and, further, results of drag reduction using 3M riblets are already available for the unswept (two-dimensional) case.[7] The results from the present work show that viscous drag reduction, which is about 8% at $\alpha = 0$ deg, progressively decreases with incidence, in contrast to the findings on two-dimensional airfoils.[5] The rapid fall in the riblet effectiveness appears to be due to significant riblet yaw-angle (φ) effects observed with an increase in incidence.

II. Experiments

A. Facility and Model

The experiments were conducted in the 1.5×1.5 m low-speed wind tunnel. The wing model, having a 13.6% thick GAW(2) profile

Received 28 March 1998; revision received 21 December 1998; accepted for publication 25 January 1999.

*Scientist, Experimental Aerodynamics Division.
†Head, Experimental Aerodynamics Division. Associate Fellow AIAA.

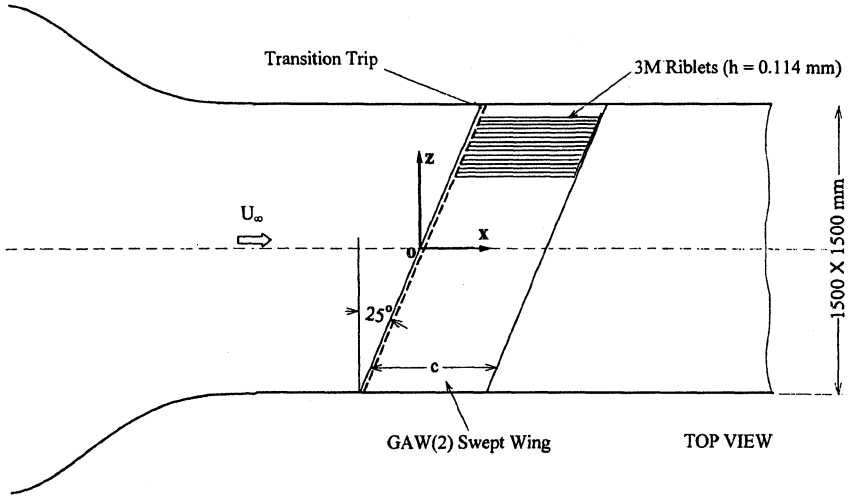

Fig. 1 Schematic of experimental setup.

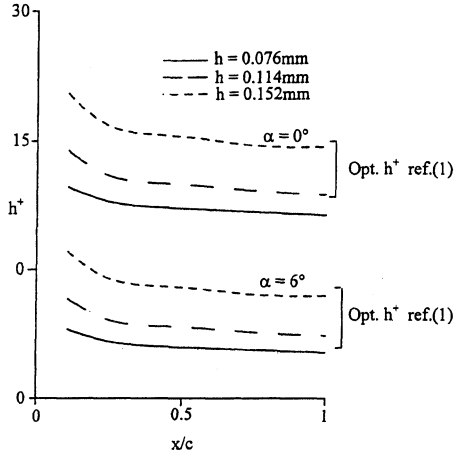

Fig. 2 Variations of h^+ on airfoil upper surface.

with a chord of 450 mm and a sweep of 25 deg, was held horizontally between the test section walls (Fig. 1). The basic airfoil profile, which has a trailing-edge thickness ratio of 0.005 (corresponding thickness being 2.25 mm on the model scale), was modified[11] to a sharp trailing edge (by extending the airfoil by 30 mm) to avoid flow complexity because of separation at the base. The model was instrumented with 48 static-pressure taps of inner diameter 0.8 mm in the direction of the freestream on both upper and lower surfaces at the midspan section; sufficient care was exercised in piercing the static-pressure hole through the riblets surface. The likely error in the measured pressure because of the finite size of the pressure holes is estimated to be less than 0.5% of the dynamic head.[12] The boundary layers on the top and bottom surfaces of the model were tripped at 10% chord from the leading edge, using transition trip (sandpaper of width 15 mm, grade 50). The 3M riblet sheets with a height h of 0.114 mm were applied between 13% chord and 96% chord on both upper and lower surfaces, with grooves aligned along the freestream direction (Fig. 1). The rear 4% chord (18 mm) was unribbed to facilitate velocity profile measurements just ahead of the trailing edge and to avoid the ambiguity concerning the origin for the distance normal to the model surface. References 1 and 5 show that the boundary layer near the wall retains the riblet effects for a two- to three-boundary-layer thickness downstream of the riblet edge. The film covered the entire wing area in the spanwise direction, i.e., from wall to wall of the test section.

B. Selection of Riblet Height

Turbulent boundary-layer computations[13] employing the lag entrainment method of Green were made using the measured surface-pressure distribution on the airfoil to determine the variation of wall skin friction at different α. Figure 2 shows the variation of h^+ on the wing upper surface for the two extreme cases, namely, $\alpha = 0$ and 6 deg for three values of riblet height. The range of h^+ for optimum drag reduction[1] is also shown. The riblet with a height of 0.114 mm chosen for the present study is in the optimum range for viscous drag reduction (Fig. 2) over the range of α. It may also be noted that, in an earlier work on a NACA 0012 airfoil at low speeds[5] (freestream conditions being very similar to the present work), results of viscous drag reduction were essentially the same for both $h = 0.114$ and 0.152 mm.

C. Measurements

The experiments were made at a freestream velocity of 30 m/s, and the corresponding chord Reynolds number was 0.75×10^6. All pressure measurements were made using low-pressure-range Setra Transducers and Furnace Control Micromanometers. Two 48-port Scani-valves were used for measuring model pressures. All of the data were acquired and processed using a PC 486 system. The total drag of the model was determined from the pitot-static surveys in the far wake using the well-known method of Jones,[14] which has been employed in earlier work[5]; the drag calculation takes into account any small pressure difference that may exist at the probe location relative to the freestream. Typically, the repeatability during measurements using the preceding method has been very satisfactory (within $\pm 1.5\%$). The reference configuration for determining drag reduction was the smooth wing with the same transition trip but without the smooth vinyl sheet (thickness = 0.1 mm) that is sometimes employed to account for the riblet backing sheet.[1] Such a backing sheet is not available now (from the 3M Company), and furthermore, the total and viscous drag reduction quoted in the paper would in fact be marginally higher in the presence of the backing sheet. Surface flow visualization studies, using titanium dioxide with hydraulic oil and oleic acid as a wetting agent, were carried out at all of the angles of attack.

Measurements of mean velocity and streamwise velocity fluctuations in the boundary layer just ahead of the trailing edge ($x/c = 0.96$) were measured at zero incidence using a conventional single hot-wire probe having a 5-μm tungsten sensor with an active sensor length of 1 mm. The wire was oriented perpendicular to the freestream direction in the xz plane. The x-wire probe configuration used for the measurement of Reynolds shear stress was again aligned in the xy plane with the sensors at 45 deg to the freestream direction. The choice of this hot-wire orientation was considered appropriate because the wall flow angle φ in the boundary layer is small (<10 deg, to be discussed in detail in Sec. III.C) at $\alpha = 0$ deg; therefore, the dominant stresses could be measured. The hot-wire sensor length and its spacing for the x configuration were about 40–50 viscous lengths, which is higher than what is generally recommended for sublayer measurements.[15] Because the measurements were made only beyond $y^+ \sim 20$, we believe that the errors, if any, in the $\langle u' \rangle$ and $\langle u'v' \rangle$ measurements may not be significant; furthermore, the interest in the present work was to show the differences in the measured quantities with and without riblets, rather than

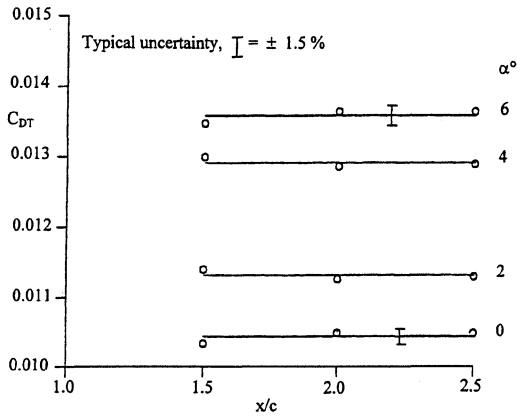

Fig. 3 Streamwise variation of total drag characteristics.

the absolute values. All of the hot-wire measurements were made using the Dantec 55M01 constant temperature anemometer with its accessories, such as the signal conditioner, digital voltmeter, rms volt meter, etc.

D. Accuracy of Measured Data

The hot-wire sensors were calibrated both before and after the measurement of each boundary-layer profile. The error in the estimation of the calibration constants for the sensors with repeated runs was within ±2%. Uncertainty in the measured data, estimated by the methodology of Kline and McClintock[16] and taking into account repeatability, are as follows:

$$\Delta C_{DT} \leq \pm 0.0015 C_{DT} \qquad (20 \text{ to } 1)$$

$$\Delta C_p \leq \pm 0.005 C_p \qquad (20 \text{ to } 1)$$

$$\Delta u \text{ m/s (hot wire)} \leq \pm 0.02u \qquad (20 \text{ to } 1)$$

$$\Delta\langle u'\rangle \leq \pm 0.04\langle u'\rangle \qquad (20 \text{ to } 1)$$

$$\Delta\langle u'v'\rangle \leq \pm 0.08\langle u'v'\rangle \qquad (20 \text{ to } 1)$$

E. Assessment of Spanwise Uniformity

On a swept-wing model, the streamlines get deflected within the boundary layer and in the near wake because of the crossflow component of the velocity vector; these effects decay rapidly and attain freestream conditions typically within one chord length from the trailing edge.[17] The spanwise uniformity of the mean flow on the wing model was therefore assessed using the well-known two-dimensional momentum integral method in the far wake as in the work of Coustols.[10] Total drag C_{DT} calculated from the measurements of pitot and static profiles at three different stations in the far wake are plotted in Fig. 3. The observation can be made that the total drag is essentially constant (within ±1.5%) at a given α, which is also the estimated uncertainty of C_{DT}; these observations suggest good mean-flow uniformity along the span over the range of α investigated.

III. Results and Discussion

A. Static-Pressure Distributions

The measured model surface-pressure distributions, both with and without riblets, at $\alpha = 0$ and 6 deg are shown in Fig. 4. As in many early studies,[5–7] the effect of riblets on surface-pressure distributions is seen to be small. The pressure drag estimated, with and without riblets at each α, showed that the difference was within 2%, with no definite trend because of riblets. The ratios of pressure drag to total drag were about 11 and 25% at $\alpha = 0$ and 6 deg, respectively; the pressure-drag values were utilized in estimating viscous drag reduction from the measured total drag reduction.

B. Drag Reduction with Riblets

The measured mean velocity profiles in the far wake (at $x/c = 2.0$, where the local static pressure was close to the freestream value) are shown in Fig. 5. From a comparison of mean velocity profiles with

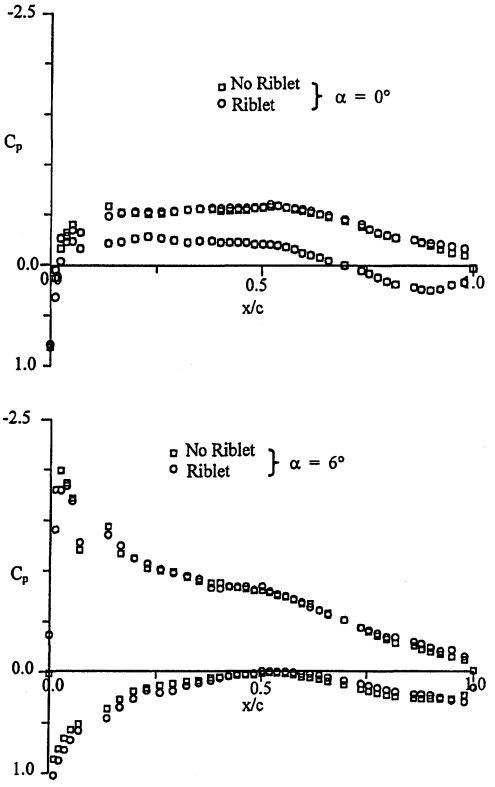

Fig. 4 Static-pressure distribution on the swept wing.

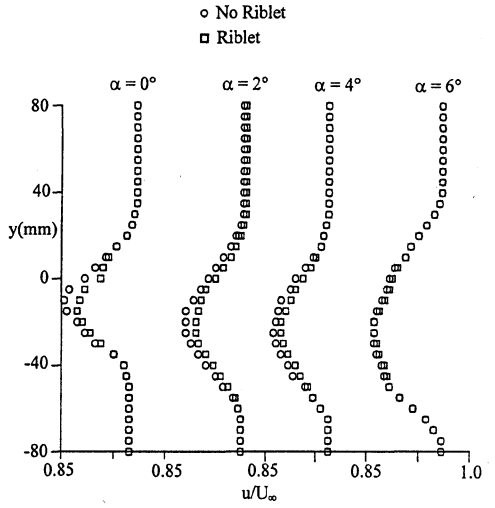

Fig. 5 Mean velocity profiles in the wake at $x/c = 2.0$.

and without riblets at a given α, we can infer that the drag reduction is maximum at $\alpha = 0$ deg and progressively reduces with increasing α. Figure 6 shows the percentage total and viscous drag reduction plotted against incidence. The normalizing factor for drag reduction at each α is the total drag for the basic airfoil configuration in the absence of riblets. The viscous drag reduction was estimated from the knowledge of pressure drag at each α. Total drag reduction of 6% and viscous drag reduction of 8% observed at $\alpha = 0$ deg are in broad agreement with the drag reduction that has been normally observed on flat-plate flows and two-dimensional airfoils at zero incidence.[1,5,6,8] Both total and viscous drag reduction progressively decrease with incidence, and viscous drag reduction is only about 1% at $\alpha = 6$ deg. The observed trend of decreasing drag reduction with incidence is in sharp contrast to the observations made earlier on two-dimensional airfoils at low speeds.[5–7]

C. Surface-Flow Visualization

Surface-flow visualization studies were undertaken primarily to provide information on riblet yaw angle φ because drag reduction

is known to be sensitive to it in two-dimensional flows.[18,19] Photographs of surface streamlines taken on the wing upper and lower surfaces at different α are displayed in Figs. 7 and 8, respectively. On the upper surface at $\alpha = 0$ and 2 deg, the surface-flow direction is practically along the freestream direction over a chordwise distance of about 60%, beyond which the flow inclination gradually increases all the way to the trailing edge. At $\alpha = 4$ and 6 deg, the features are qualitatively similar to the observations $\alpha = 0$ and 2 deg, except that the surface streamlines begin to deviate (from the freestream direction) around 25–30% chord and even more significantly toward the trailing edge. The flow patterns on the lower surface also show features of deviation of surface flow from the freestream direction but in the opposite direction (to those observed on the upper surface), particularly at $\alpha = 0$ deg, and a reversal in trend toward the trailing edge.

The results of surface-flow inclination angle φ with respect to the riblet orientation, inferred from the preceding flow-visualization pictures, are plotted against streamwise distance for both and upper and lower surfaces in Fig. 9. As already discussed, at $\alpha = 0$ and 2 deg on the upper surface, φ is less than 5 deg over a large fraction of the chord and increases to about 15 deg toward the trailing edge; on the other hand, at $\alpha = 4$ and 6 deg, φ increases rapidly beyond $x/c \sim 0.60$ and reaches values as high as 27 deg at $\alpha = 6$ deg over a sizable portion of the chord. On the lower surface, although the magnitude of φ is well within 15 deg, a large part of the wing chord (about 75%) is affected by φ effects, with a reversal of surface-flow direction toward the trailing edge.

D. Possible Explanation for Fall in Effectiveness of Riblet Performance with Incidence

Earlier work on flat-plate, boundary-layer flows and bodies of revolution assessing φ effects on riblet performance indicate that both the magnitude of drag reduction and the (max) value of h^+ up to which drag reduction is retained are sensitive to φ. For example, in the work of Coustols[18] employing 3M riblets, for $\varphi = 20$ deg, the observed drag reduction was significantly reduced from 10 to 3% at $h^+ \sim 10$, with zero drag-reduction crossover reduced to $h^+ \sim 12$ from $h^+ \sim 20$. On the axisymmetric body at zero α (Ref. 18), the maximum drag reduction dropped from about 7 to 3% at $\varphi = 20$ deg. The data of Walsh and Lindermann[19] showed about a 5% drop in drag reduction up to $\varphi = 15$ deg but showed a drag increase at $\varphi = 30$ deg; in fact, there was a significant increase in drag (about 15%) beyond $h^+ = 10$ for $\varphi = 30$ deg. With the limited data

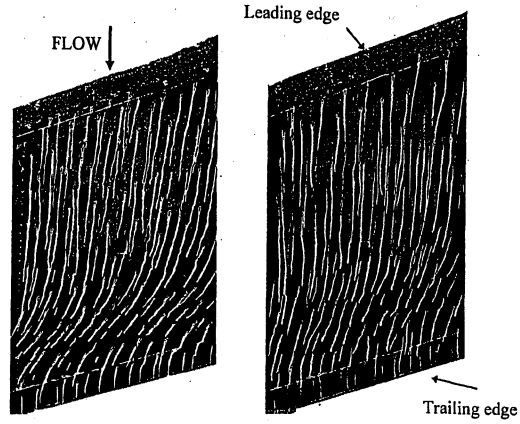

a) $\alpha = 0$ deg b) $\alpha = 6$ deg

Fig. 8 Streamline patterns on the lower surface.

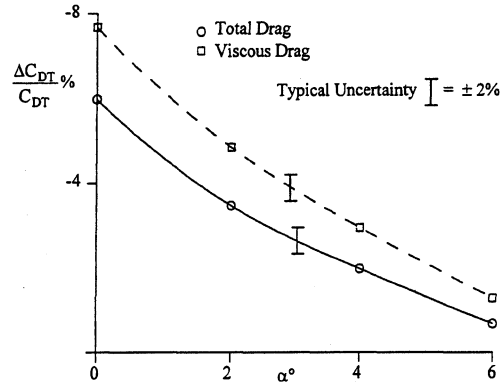

Fig. 6 Drag reduction because of riblets with incidence.

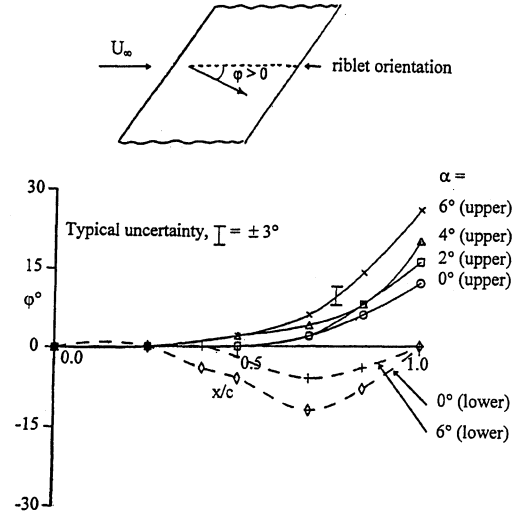

Fig. 9 Streamwise variation of riblet yaw angle with incidence.

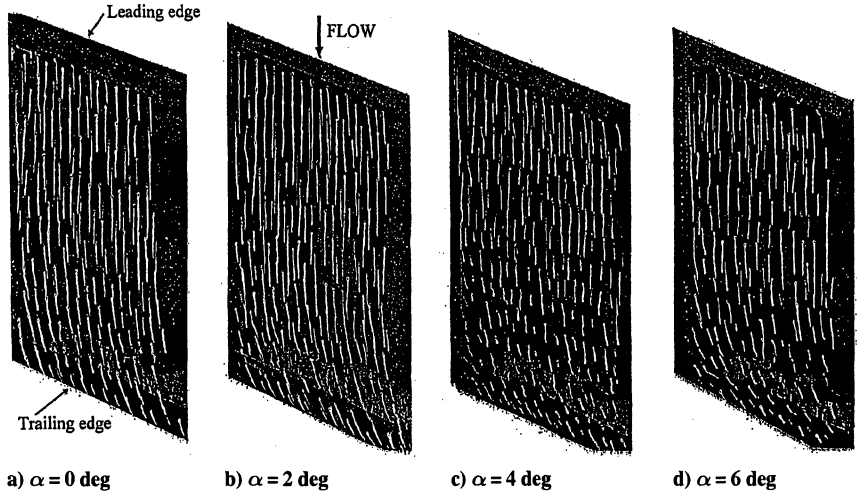

a) $\alpha = 0$ deg b) $\alpha = 2$ deg c) $\alpha = 4$ deg d) $\alpha = 6$ deg

Fig. 7 Streamline patterns on the upper surface.

available, it may be reasonable to assume that drag reduction is limited to $\varphi < 15$ deg.

In the present work on a swept wing, φ effects are associated with crossflow boundary layers as well, unlike the earlier studies of two-dimensional flows examining the φ effect alone. The magnitude of viscous drag reduction observed at $\alpha = 0$ deg (about 8%, which is comparable to the values generally observed on a two-dimensional flat plate and airfoil at zero incidence[1,5]) strongly suggests that riblet effectiveness on a swept wing is not much affected, as long as $\varphi \leq 15$ deg over a large part of the wing chord. Such a suggestion is in fact broadly consistent with the riblet yaw angle effect observed in two-dimensional flows.[18,19] We suspect that the falling trend of drag reduction observed at higher incidence in the present tests is associated with larger values of φ (>15 deg) observed beyond about 50% chord on the wing upper surface. Because there is evidence that viscous drag reduction is contributed to appreciably by the upper surface of the airfoil in two-dimensional flows,[5] the relatively large values of φ observed (Fig. 9) on the wing upper surface could be primarily responsible for the significant reduction in riblet effectiveness at higher α. As we shall see in the next section, as on two-dimensional airfoils, the wing upper surface is the major contributor to the drag reduction in the swept case as well.

E. Boundary-Layer Properties Ahead of the Trailing Edge

From all of the preceding measurements, the riblets are evidently quite effective at $\alpha = 0$ deg even under the influence of (relatively small) yaw-angle effects as a result of the three-dimensional boundary layer on the swept wing. Measurements of mean velocity, streamwise velocity fluctuations, and Reynolds shear-stress distributions were made just ahead of the trailing edge to get additional information on the boundary-layer properties under the influence of the riblets.

The mean velocity profiles measured (at $x/c = 0.96$) on both upper and lower surfaces at $\alpha = 0$ deg are shown in Fig. 10. On the upper surface, riblets lead to a relatively higher velocity over a sizable part of the boundary layer as in two-dimensional flows.[4,5] On the other hand, the velocity profiles on the lower surface show a very weak effect because of riblets. These results again suggest that a major contribution to drag reduction results from the upper surface of the wing.

The streamwise turbulence intensity profiles in the boundary layer on the upper and lower surfaces measured at $x/c = 0.96$ are shown in Fig. 11. The results show a reduction in the turbulence intensities (about 8%) from riblets in the near-wall region. On the other hand, there is no observable reduction in the intensities on the lower surface with riblet. The power spectra of the u' near the wall ($y^+ \sim 20$) on the upper surface (shown in Fig. 12) indicate a reduction in energy levels at low frequencies (below 200 Hz) on the riblet surface. All of the preceding features are qualitatively similar to those observations on two-dimensional flows.[5]

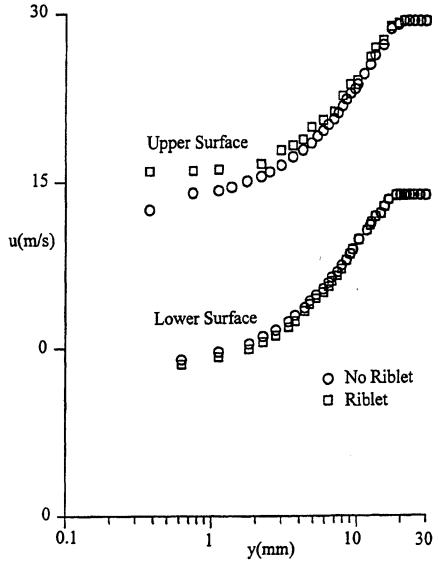

Fig. 10 Mean velocity profiles ahead of the trailing edge at $\alpha = 0$ deg.

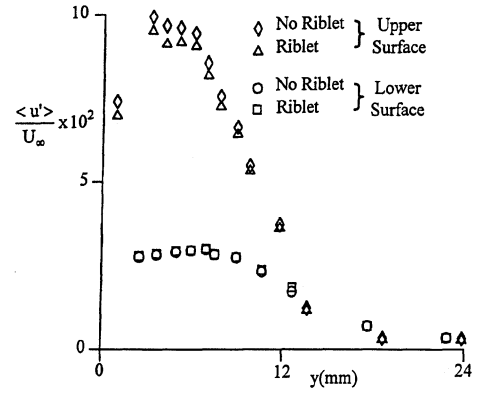

Fig. 11 Streamwise turbulence intensity profiles at $\alpha = 0$ deg.

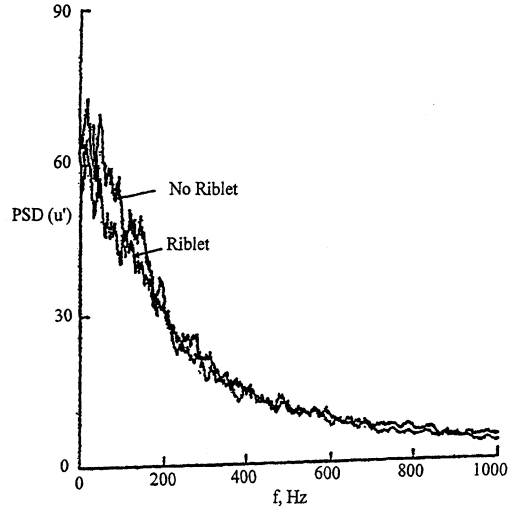

Fig. 12 Power spectral density of streamwise turbulent fluctuation at $\alpha = 0$ deg.

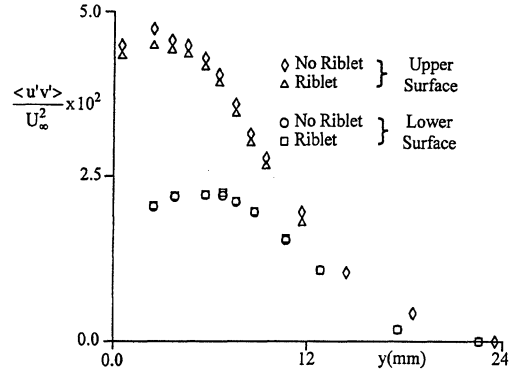

Fig. 13 Reynolds shear-stress profiles at $\alpha = 0$ deg.

Figure 13 shows the variation of Reynolds shear stress $\langle u'v' \rangle$ across the boundary layer for both upper and lower surfaces. Reduction in the shear stress because of riblets (about 8%) in the wall region of the upper surface can be observed, whereas no such reduction is seen on the lower surface, which is very similar to the riblet effect on u' distributions (Fig. 12). Although the likely errors in $\langle u'v' \rangle$ can be as much as 8%, the data exhibit a definite trend. These results are once again similar to those obtained in two-dimensional flows at zero incidence.[5]

IV. Conclusions

Detailed experiments have been performed assessing viscous drag reduction employing riblets on an infinite swept wing at low speeds.

The wing utilized for the study had a GAW(2) profile and a sweep of 25 deg. The tests were made at a chord Reynolds number of 0.75×10^6 and covered an incidence range of 0–6 deg. The results showed maximum total and viscous drag reductions of 6 and 8%, respectively, at zero incidence, which are comparable to those observed on two-dimensional flat plates and airfoils. With an increase in α, a rapid fall in effectiveness of riblets was noted, with a viscous drag reduction of about 1% at $\alpha = 6$ deg. The results from surface-flow visualization studies on the swept wing and a comparison with riblet yaw-angle φ effects studied in two-dimensional flows strongly suggest that the rapid fall in riblet effectiveness with increasing α is associated with significant φ effects observed, particularly on the wing upper surface. In essence, the results indicate that the riblet effectiveness is not greatly impaired in the presence of a crossflow boundary layer, as long as the riblets' yaw angles are well within 15 deg over a large part of the wing chord. We may, in general, expect that both the magnitude of φ and its streamwise gradients will be relevant factors affecting riblet performance in three-dimensional, boundary-layer flows.

Measurements of streamwise turbulent intensity and Reynolds shear-stress profiles measured just ahead of the wing trailing edge at zero incidence showed a reduction near the wall in the presence of riblets, similar to the effects observed on two-dimensional airfoils.

In summary, the results stress the importance of aligning the riblets along the local surface streamline direction on a swept wing (for example, corresponding to cruise conditions) to fully realize the benefits of riblet action.

Acknowledgments

Excellent assistance and warm cooperation rendered by the staff of the 1.5-m and boundary-layer tunnels are gratefully acknowledged.

References

[1]Walsh, M. J., "Riblets," *Viscous Drag Reduction in Boundary Layers*, edited by D. M. Bushnell and J. N. Hefner, Vol. 123, Progress in Astronautics and Aeronautics, AIAA, Washington, DC, 1990, pp. 203–261.

[2]Vukoslavcevic, P., Wallace, J. M., and Balint, J. L., "On the Mechanism of Viscous Drag Reduction Using Streamwise Aligned Riblets—A Review with New Results," Royal Aeronautical Society International Conf. on Turbulent Drag Reduction by Passive Means, Royal Aeronautical Society, London, Sept. 1987.

[3]Coustols, E., and Savill, A. M., "Turbulent Skin Friction Drag Reduction by Active and Passive Means," AGARD 786, 1992.

[4]Choi, K. S., "Near-Wall Structure of Turbulent Boundary Layer with Riblet," *Journal of Fluid Mechanics*, Vol. 208, No. 11, 1989, pp. 417–458.

[5]Sundaram, S., Viswanath, P. R., and Rudrakumar, S., "Studies of Turbulent Drag Reduction Using Riblets on a NACA 0012 Airfoil," *AIAA Journal*, Vol. 34, No. 4, 1996, pp. 676–682.

[6]Subaschandar, N., Kumar, R., and Sundaram, S., "Drag Reduction Due to Riblets on NACA 0012 Airfoil at Higher Angles of Attack," National Aerospace Labs., Rept. PD-EA-9504, Bangalore, India, March 1995.

[7]Subaschandar, N., Kumar, R., and Sundaram, S., "Drag Reduction Due to Riblets on GAW(2) Airfoil," National Aerospace Labs., Rept. PD-EA-9601, Bangalore, India, March 1996; also *Journal of Aircraft* (to be published).

[8]Viswanath, P. R., and Mukund, R., "Turbulent Drag Reduction Using Riblets on a Supercritical Airfoil at Transonic Speeds," *AIAA Journal*, Vol. 33, No. 5, 1995, pp. 945–947.

[9]Mclean, J. D., George-Falvy, D. N., and Sullivan, P. P., "Flight Tests of Turbulent Skin Friction Reduction by Riblets," *Proceedings of International Conference of Turbulent Drag Reduction by Passive Means*, Sec. 16, Royal Aeronautical Society, London, 1987, pp. 1–17.

[10]Coustols, E., "Control of Turbulence by Internal and External Manipulators," *Applied Scientific Research*, Vol. 46, No. 3, 1989, pp. 183–196.

[11]Sundaram, S., Viswanath, P. R., and Subaschandra, N., "Studies on Drag Reduction Using Riblets on an Infinite Swept Wing," National Aerospace Labs., Rept. PD EA-9802, Bangalore, India, March 1998.

[12]Chue, S. H., "Pressure Probes for Fluid Measurement," *Progress in Aerospace Sciences*, Vol. 16, No. 1, 1975, p. 188.

[13]Desai, S. S., and Kiske, S., "A Computer Program to Calculate Turbulent Boundary Layer and Wakes in Compressible Flow with Arbitrary Pressure Gradient Based on Green's Lag Entrainment Method," Rept. Br. 89/1982, Institut für Thermo- und Fluiddynamik, Ruhr Univ., Bochum, Germany, 1982.

[14]Schlicting, H., *Boundary Layer Theory*, 7th ed., McGraw–Hill, New York, 1979, p. 711.

[15]Ligrani, P. M., and Bradshaw, P., "Spatial Resolution and Measurement of Turbulence in the Viscous Sublayer Using Subminiature Hot Wire Probes," *Experiments in Fluids*, Vol. 5, No. 6, 1987, pp. 407–417.

[16]Kline, S. J., and McClintock, F. A., "Describing Uncertainties in Single Sample Experiments," *Mechanical Engineering*, Vol. 75, No. 1, 1953, pp. 3–8.

[17]Coustols, E., "Performance of Internal Manipulations in Subsonic 3D Flows," *Recent Development in Turbulence Management*, Vol. 6, edited by K. S. Choi, Kluwer Academic, Norwell, MA, 1991, pp. 43–64.

[18]Coustols, E., "Behaviour of Internal Manipulators: 'Riblet' Models in Subsonic and Transonic Flows," AIAA Paper 89-0963, 1989.

[19]Walsh, M. J., and Lindemann, M., "Optimization and Application of Riblets for Turbulent Drag Reduction," AIAA Paper 84-0347, 1984.

J. C. Hermanson
Associate Editor